100→111 Morphological Change on KCl Crystals Grown from Pb2+doped aqueous solutions

Journal Name

ARTICLE

{100}→{111} Morphological Change on KCl Crystals Grown from Pb^{2+} doped aqueous solutions

Received 00th January 20xx,
Accepted 00th January 20xx

DOI: 10.1039/x0xx00000x

www.rsc.org/

L. Pastero,[a] R. Cossio [a] and D. Aquilano[a]†

KCl f.c.c. crystals generally exhibit {100} habit when growing from pure aqueous solutions, a richer {100} + {111} morphology being obtained only under well-defined growth temperature and supersaturation. When increasing amounts (less than 2000 ppm) of Pb are put in supersaturated solution, the KCl growth morphology undergoes a progressive change: {100} → {100} + {111} → {111}. Detailed growth patterns have been investigated by means of SEM and AFM, while EDS and XRF analyses allowed to ascertain that Pb is not only adsorbed on the growing KCl surfaces, but also selectively absorbed within the {111} growth sectors. Starting from recent and analogous findings, we tried to interpret the morphological change by means of a geometric and structural model of epitaxy between the {100} and {111} forms of KCl and the most important forms of those compounds that could be adsorbed on them: $PbCl_2$ (cotunnite), PbCl(OH) (laurionite-paralaurionite) and $KCl{\cdot}PbCl_2$ (challacolloite). Excellent lattice coincidences have been found, so proving that the {111} KCl octahedron is largely privileged for adsorption/absorption to occur with respect to the {100} KCl cube. Based on this ground, simple kinetic considerations can be proposed to satisfactorily explain the observed morphology change.

Introduction

Ninety years ago Gaubert[1] first suggested that the habit change of a crystal and the oriented deposit of crystals of a given species, on a crystal of a different species, are nothing else than two phenomena generated by the same cause. Bunn[2] and Royer[3a-e] tried to verify this hypothesis. Royer, investigating crystals with simple and well known structure, first demonstrated that a habit change should occur when the 2D lattices of the new appeared face and the one of the "crystallizing impurity" show close parametric size.

Starting from the findings by Retgers,[4] Royer hypothesized that the {100} → {100} + {111} habit change underwent by KCl crystallizing in the presence of $PbCl_2$ occurred because "… the 2D lattice cell of the new {111} form shows the same size of the 2D cell of one of the faces of the crystalline impurity introduced in the mother phase…". As a matter of fact, the original Royer's intuition was that the ratio (b_0/a_0)=1.706 between the cell parameters on the 001 plane of the orthorhombic $PbCl_2$ is very close to the value √3=1.732 which represents, in turn, the parametric ratio of the rectangular cell that can be determined on the 111 plane of the KCl crystal. In other words, Royer outlined that the pseudo-hexagonal symmetry of the {001} form of $PbCl_2$ fits with the trigonal one of the KCl-{111} octahedron, so favoring the {100} → {111} habit change.[3d,e] The same reasoning was applied to interpret the {100} → {111} morphological transition of both KBr and KI crystals growing in the presence of the orthorhombic $PbBr_2$ and of the hexagonal PbI_2, respectively. However, the coincidence between host and guest lattices is a necessary but not sufficient constraint to obtain a change of habit, as shown by Royer itself.[3c]

It has been also well known that the {100} + {111} habit change of KCl and NaCl crystals in the presence of minor amounts of Pb ions in aqueous solution was recorded in two-dimensional diagrams (supersaturation vs impurity concentration) called "morphodromes", obtained on both growth[5-8] and dissolution morphology[9] through in situ and ex-situ observations.

Later on,[10] careful in-situ observations showed that in KCl crystals grown from pure aqueous solution the {100} form exhibits square growth layers bounded by straight <001> steps, when the relative supersaturation of solution, $\sigma=(c_{solution}/c_{saturation})-1$, is lower than 0.01 and it transforms to a hopper-form when σ reaches 0.015; here $c_{solution}$ and $c_{saturation}$ represent the concentration of the solution at supersaturation and saturation, respectively. In the presence of Pb ions the <001> steps become less stable and truncated by diagonal <110> steps; further, the advancement rate of the steps decreases whereas their height increases with the Pb concentration. Thus, the {111} octahedron starts to appear, in the presence of Pb ions, associated with the appearance of the <110> steps on the cube faces. The earlier stages of the octahedron occurrence are followed by the appearance of growth layers on the octahedron surfaces originating

[a] Dipartimento di Scienze della Terra, Università degli Studi, via Valperga Caluso 35, I-10125, Torino, Italy.
† To whom correspondence should be addressed: dino.aquilano@unito.it
Electronic Supplementary Information (ESI) available: [details of any supplementary information available should be included here]. See DOI: 10.1039/x0xx00000x

alternately from opposite corners or edges of the face. Successively, growth spirals start to appear from the central portion of the octahedron faces and their step become thicker with increasing Pb concentration in the mother solution. The overall growth morphology is summarized in Fig. 1 where both crystal habit and surface micromorphology are represented as a function of the solution supersaturation and Pb concentration.[10]

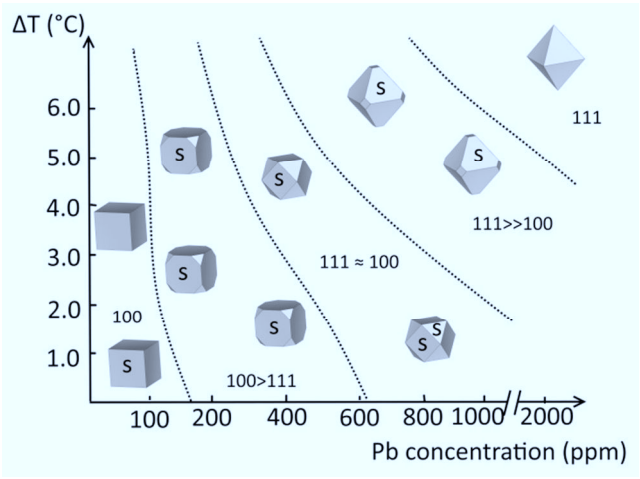

Figure 1. Morphodrome of KCl crystals growing at different supersaturation values and under different Pb concentration (ppm) in solution; label ***s*** indicates the presence of growth spirals on the growing faces. Inspired and elaborated from reference 10. See S.I., Fig. 1 for details.

Epitaxial growth experiments were carried out on KCl seed crystals, having initial {100}+{111} habit, immersed in a KCl+$PbCl_2$ solutions where the concentration of Pb ions ranged from 0.8 to 1% . It was observed that "…small crystallites with an elongated prismatic habit corresponding to the one of $PbCl_2$ crystals, grew in epitaxial orientation on {111}, and less clearly on {100} faces. On both faces, the elongation of $PbCl_2$ crystallites is parallel to the set of <110> directions of KCl. The epitaxial relation between $PbCl_2$ and KCl is thus confirmed". Based on this argument, it was concluded that "…the habit change of KCl crystals, from cubic to octahedral, obtained in the presence of Pb ions in solution, takes place probably because the Pb ions precipitate in the form of $PbCl_2$ crystallites preferentially along the <110> steps of the growth layers running on the {100} flat faces. This reduces the advancing rate of the growth layers and results in a piling-up of <110> steps; hence, the originally kinked {111} form (K-type, in the sense of Hartman-Perdok[11]) changes to a stepped form (S-type[11]). As a result, small {111} faces appear that become larger by the spiral growth mechanism.[10]

Unfortunately, the epitaxial growth of $PbCl_2$ crystallites along the <110> directions of KCl was not proved by means of photographic evidence.

In the present paper, KCl crystals were nucleated and grown from aqueous solutions in the presence of increasing Pb concentrations (from 0 to 2000 ppm), under controlled crystallization temperature and supersaturation, with the aim at determining the mechanisms ruling out the morphological transition: {100}→{100}+{111}. Keen attention is paid to the reticular relationships between the {111}-KCl substrate and the adsorbed matter that could deposit on it, in the form of epitaxial 2D-phases related to those 3D-phases, like $PbCl_2$ (cotunnite), PbCl(OH) (laurionite, para-laurionite) and $KCl{\cdot}2PbCl_2$ (challacolloite), which could potentially precipitate in the growth solution under suitable supersaturation conditions. We are confident in this epitaxial approach, owing to the recent examples of habit change we found on the following epitaxial couples: Li_2CO_3 (zabuyelite) / $CaCO_3$ (calcite),[12] $BaCO_3$ (witherite) / SiO_2 (quartz)[13a,b] and NaCl / H-CO-NH_2 (formamide).[14]

Experimental

Cubic-octahedral KCl crystals were obtained following two growth routines: the first, to compare the results with those of Liang et al.,[10] involves growth experiments performed, starting from KCl (Sigma-Aldrich analytical grade) aqueous solutions saturated at 40°C (solubility 40.05 g/100g water), by repeated crystallization from a starting temperature of 95°C. According to the second routine, crystals were grown from a KCl solution saturated at 25°C and cooled down to 4°C, in the presence of variable amount of $PbCl_2$. The Pb^{2+} concentration was adjusted from 0 to 2000 ppm, adding both analytical grade solid $PbCl_2$ or $Pb(CH_3COO)_2{\cdot}3H_2O$. Lead acetate was chosen because of its higher solubility with respect to lead chloride and in order to reduce the chlorine concentration in the starting solution, so avoiding the common-ion effect. Moreover, its chelating properties are useful to limit the precipitation of crystalline $PbCl_2$ when lead concentration rises and, consequently, to preserve the requested lead concentration. Chelating substances must be used being aware of their effect as habit modifiers. Aiming at excluding the eventual surface poisoning effect due to the presence of acetate ions in solution, all experiments were carried both in pure chloride and acetate solutions. KCl precipitation was induced by cooling down the solution to 34°C, in order to reproduce and compare our results with those published by Lian et al.[10] and obtained at relative supersaturation σ = 0.03, by imposing a temperature gradient ΔT=6°C. We adopted as well the same starting temperature and Pb^{2+} concentrations chosen by Lian et al. to relate the habit changes of KCl to the σ value and to the Pb concentration.

Experiment code	$T_{saturation}$ (°C)	T_{growth} (°C)	Pb^{2+}/K^{+} molar ratio
KPC	40	34	0 - 0.0013
nKPC	25	4	0 - 0.0015

SEM – AFM Imaging and EDS analysis

The overall crystal morphology was observed by means of a Scanning Electron Microscope Cambridge S-360 (EHT 30 kV, wd 5mm, current probe 100 pA). An Electron Dispersion Spectrometer Oxford INCA Energy 200 was used to get the

qualitative elemental mapping (EHT 15 kV, wd 25mm, current probe 2.5 nA). Surface detailed morphology was observed by Atomic Force Microscopy using a DME Dual Scope Microscope (alternated contact mode, silicon nitride Au coated probes with typical resonant frequency 170 kHz and typical force constant 40 N/m).

XRF analysis

The elemental composition of some samples was mapped using an EDAX Eagle-III XPL µProbe, the instrument being equipped with a Rh X-ray tube and X-ray Poly-capillary Lens with a spot size of 30µm. The working conditions were 40kV and 1mA, Ti 25 µm thick primary filter, resolution 128x100 pixels, dwell time=4s.

A KCl crystal grown from a cooled solution containing 500 ppm of Pb^{2+} ($PbCl_2$) was used in order to obtain the Pb distribution inside the crystal. The crystal as grown, showed well-developed cube faces and small complementary octahedron faces, corresponding to extended growth sectors of the cube and narrow growth sectors of the octahedron. The crystal was dry-polished in order to ensure the planarity of the surface to be mapped. KK, ClK and PbL lines were used.

The Pb distribution is shown in Figure 2. As one can observe, the Pb concentration is higher within the growth sectors of the octahedron and shows an oscillatory behavior mainly during the first stages of growth (close to the center of the crystal). In correspondence of the growth sectors of the cube the concentration of lead is smooth and quite uniform, decreasing during the late stages of growth. The Pb distribution in the crystal bulk is related to the preferential absorption on the surfaces of the octahedron. This leads to a rise of lead concentration inside the octahedron growth sectors, since adsorption/absorption occurs onto the octahedron terraces. On the contrary, the smooth distribution inside the cube sectors is due to the lack of Pb absorption onto the cube terraces. Here the absorption could occur only on the ledges

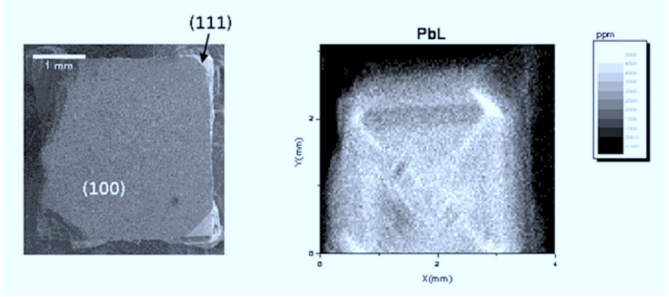

Figure 2. The SEM image of the sample, used as a morphological reference for the Pb distribution inside the crystal (left side). Pb concentration, in ppm (right side).

of the macrosteps running on the cube faces and having the structure of the octahedron facets, as it will be detailed in following chapter.

KCl crystals grown in the presence of Pb ions: the overall morphology

As expected, the simply cubic habit observed in pure aqueous solution progressively changes to {100}+{111} and then to the dominating {111}, as much as c_{Pb} increases (Fig. 3).

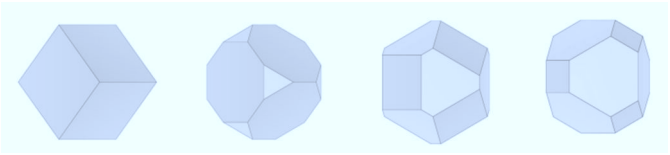

Figure 3. Observed habit of KCl grown (ΔT=6°C) in the presence of increasing percentage (c_{Pb}) of Pb ions in solution. From left to right: c_{Pb} = 0, 500, 1000, 2000 ppm. {100}, grey color; {111}, orange. The {111} form increases its importance with c_{Pb} .

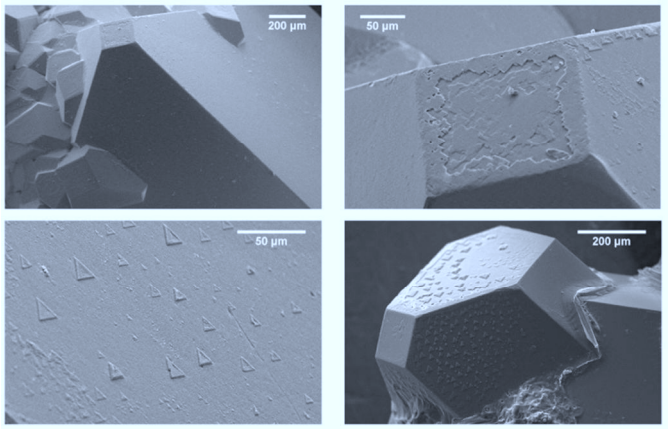

Figure 4. SEM images of KCl crystals grown from Pb doped solutions. The octahedron dominates the cube (top-left). The surface growth pattern of a cube face is made by layers running parallel to the diagonals of the face, i.e. by <100> macrosteps (top-right). Trigonal 3D islands nucleate on the octahedron faces: the filling up of the islands starts from their periphery (bottom-left). Islands, once completely filled, show their terraces parallel to the {111} substrate (bottom-right).

From the overall surface patterns of both cube and octahedron faces it follows that:

i) On the cube faces, the lead presence induces, even at a low concentration, patterns built by <100> macrosteps which are nothing else than thin ledges having the slopes of the anticlockwise sequence of the cube faces: (100), (010) and (001), as detailed in the S.I., Fig.2 left. It is worth noting as well that, contrary to Lian *et al*. conclusions,[10] the presence of $PbCl_2$ crystallites aligned along the <100> macrosteps is excluded (Fig. 4 top).

ii) The surfaces of both {100} and {111} forms don't show growth spirals, at SEM resolution level.

iii) Beyond a critical supersaturation, growth islands appear on the octahedron only. These 3D hillocks are regularly oriented with respect to the face edges. As

shown in Fig. 4 (bottom), they show trigonal symmetry, according to the surface symmetry of the KCl octahedron. When labelling as (111) one of the octahedron faces, then every hillock is laterally limited by very thin (100), (010) and (001) micro-facets and is truncated by a (111) terrace (see details in S.I., Fig.2 right).

The difference between the surface patterns of our crystals and those obtained by Lian et al. (dominated by growth spirals) is striking but not surprising. In fact, it is likely that our crystals, free falling in the mother solution and hence exempt of severe mechanical constriction, result to be poorly dislocated; on the contrary, cutting and polishing the KCl seeds for both growth and dissolution experiments, had surely introduced stresses, and hence linear defects in the Lian crystals.

The detailed surface patterns of the {111} form grown in the presence of Pb ions.

When looking more closely at the as grown {111} form, detailed features do appear disclosing the early stages of advancement of its surfaces (Fig. 5).

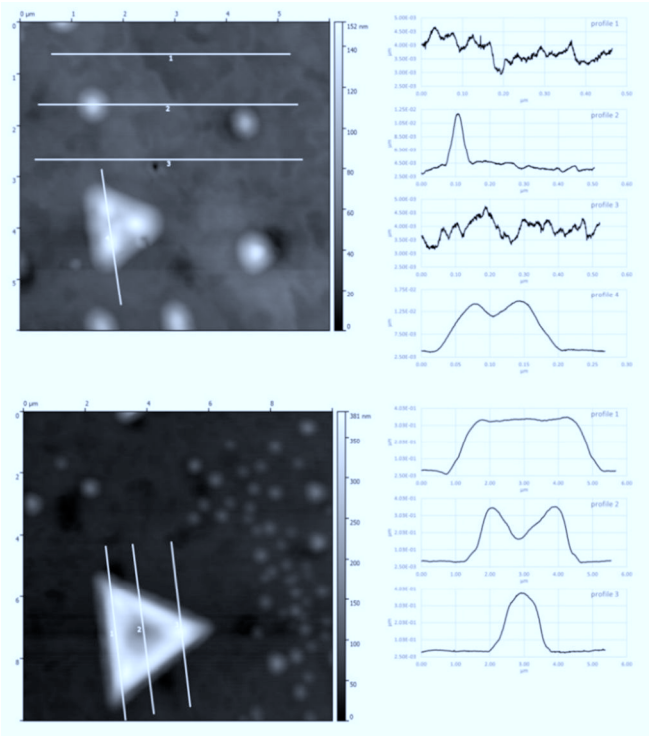

Figure 5. Early stages of the patterns observed on the {111} KCl form grown in the presence of Pb ions (AFM pictures). Single and triple KCl hillocks emerging on a rough surface (top left). The corresponding profiles are referred to a single hillock and to the averaged thickness (15 nm) of the rough surface (top right). A triple hillock (bottom left) shows a complex morphology, as follows from the profiles obtained from three different and parallel cuts (bottom right).

Single hillocks actually look as truncated triangular pyramids: they are very flat, the lateral extension reaching ~750 nm while their height does not exceed 75 nm.

The shape of the triple hillocks outlines the triangular symmetry of the pyramids, while the profiles of their cuts (Fig.5, bottom right) allow to reveal their growth mechanism. Lateral size reaches ~6000 nm, the mean height being 200 nm. The terrace of the hillocks shows the maximum height at the three corners (~300 nm); the height decreases to 250 nm (midway between two corners) and finally, to 150 nm, at the center of the hillocks.

When summarizing, a careful analysis of the 3D profile of the hillocks suggests:

i) The advancement rate of the hillock terraces is the highest one at the corners, slows down at the terrace borders and reaches its minimum value in its central part: this kinetic behavior depends unambiguously on the volume diffusion (around the hillock) which dominates in absence of an hydrodynamic regime. As a matter of fact, our crystals grow in a quasi-stagnant mother solution: thus, the concentration gradient in solution (i.e. the supersaturation) results to be maximum at the corners and minimum on the middle of the terraces.

ii) As much as the size of a growing hillock increases, the aspect ratio (*h/l*) between its height (*h*) and the corresponding lateral size (*l*) decreases. This proves that the {100} micro-facets, that laterally limit a hillock, advance more rapidly than the hillock top which is parallel to the {111} surfaces.

iii) From ii) it follows that, since the early stages of the surface nucleation, the {111} form is much more affected by Pb adsorption than {100}. It is worth here remembering that, in pure aqueous solution: a) the equilibrium shape of alkali halides with NaCl–lattice type shows the {100} form only;[15] b) the growth shape exhibits the {111} form within a narrow domain of temperature and supersaturation.[16] Accordingly, a complex question arises:

- Is the random poisoning of the surface kinks which is responsible of the strong anisotropy of Pb adsorption on the cube and octahedron faces?
- Otherwise, is the Pb adsorption on the ledges, running on both the {100} and {111} surfaces, which generates the difference in their advancement rate?
- Finally, can set up perhaps an ordered Pb adsorption on the {111} surfaces? This could occur by means of shaped like 2D epitaxial islands nucleating from the mother solution, which is obviously supersaturated with respect to KCl but surely unsaturated with respect to the 3D phases that could crystallize, such as $PbCl_2$, PbCl(OH) and $KCl{\cdot}2PbCl_2$.

First of all, to face this path one should consider that a crystal face can grow, in a chemically closed system, only if it already existed on the shape of the critical 3D crystal embryo, at nucleation. In our case, this could occur only if the value of the specific surface energy of the {111}-KCl form is lowered to such a degree that {111} faces enter the 3D equilibrium shape of

the crystal.[17] Then, we hypothesized that the temporary epitaxy of one, or more, of the potentially crystallizing phases in the Pb-doped growth solution could allow the {111} form to be stabilized since the early stages of nucleation.
Geometric and structural conditions for these epitaxies will be searched in this work, while surface energy calculation to confirm the epitaxial way will be the subject of a forthcoming paper.

Geometric and reticular conditions for epitaxy on {100} and {111}-KCl forms growing from Pb-doped aqueous solutions.

The most common compounds that can crystallize, at room temperature and pressure, in aqueous solutions containing K, Cl and Pb are: $PbCl_2$ (Cotunnite), PbCl(OH) (Laurionite, Para-Laurionite) and $KCl{\cdot}2PbCl_2$ (Challacolloite), as shown in Table 1, where the lattice parameters are reported with the error bars, when available in the original papers.

Substrate	a_0	b_0	c_0	β (°)	Space group	Mineral name
KCl	6.293				Fm3m	Sylvite
Potential epitaxial deposits						
$PbCl_2$	7.622	9.045	4.535		Pnam	Cotunnite [21, 22]
PbCl(OH)	9.6987(15)	4.0203(8)	7.1110(9)		Pcmn	Laurionite [21, 22]
PbCl(OH)	10.865(4)	4.006(2)	7.233(3)	117.24(4)	C2/m	Para-Laurionite [25]
$KCl{\cdot}2PbCl_2$	8.864(8)	7.932(8)	12.491(11)	90.153(5)	$P2_1/c$	Challacolloite [26]

Table 1. Lattice parameters (Å), space groups and mineral names of the potential compounds that could epitaxially deposit on {100} and {111}-KCl form.

Starting from the bulk structures we searched for their 2D-lattice coincidences on both {100} and {111}-KCl forms, as shown in Table 2, 4 and 5, respectively. The vectors defining the 2D coincidence cells (column 2 and 4, length in Å) at the host/guest interfaces are chosen in order to minimize their linear misfit (column 5). The 2D-areas ($Å^2$) refer to the coincidence cells; we think that this quantity is worth to be considered for every kind of a bi-crystal interface (epitaxy, twinning) since lower the multiplicity of the coincidence cell (column 6) higher the interface stability. Finally, d_{hkl} thicknesses (Å) refer to the elementary host/guest layers potentially making epitaxy; their misfits are not relevant for epitaxy to occur, but play a fundamental role to allow an epitaxially adsorbed layer to transform into an absorbed one.[12,14]

The KCl /$PbCl_2$ interfaces

Crystal form (host) KCl	2D-lattice of the host form	Crystal form (guest) $PbCl_2$	2D-lattice of the guest form	2D- misfit (host/guest) Δ%	Notes
{100}	$[1\bar{1}0]$ = 8.899	**{001}**	[100] = 7.622	– 16.76	Δ% exceeds the limits of 2D epitaxy
	[110] = 8.899		[010] = 9.045	+ 1.63	Low misfit
2D area	79.206		68.941	–14.90	Δ% exceeds the limits of 2D epitaxy
	d_{200} =3.146		d_{002} = 2.267	–38.77	
{100}	$[1\bar{1}0]$ = 8.899	**{010}**	2×[001] = 9.069	+ 1.91	
	[110] = 8.899		[100] = 7.622	– 16.76	Δ% exceeds the limits of 2D epitaxy
2D-area	79.206		69.130	– 14.57	Δ% exceeds the limits of 2D epitaxy
	d_{200} = 3.146		d_{020} = 4.572	+45.31	
{100}	$[1\bar{1}0]$ = 8.899	**{100}**	2×[001] = 9.069	+1.91	Low misfit, but the d_{200} slices of ($PbCl_2$) are highly wavy
	[110] = 8.899		[010] = 9.045	+1.63	Low misfit
2D area	79.206		82.033	+ 3.57	Low multiplicity of the common cell = 2×(100)KCl
	6×d_{200} =18.876		5×d_{200} = 19.055	+0.95	Absorption difficult to be obtained
{100}	$[1\bar{1}0]$ = 8.899	**{101}**	$[10\bar{1}]$ = 8.853	– 0.53	Very low misfit
	[110] = 8.899		[010] = 9.045	+1.63	Low misfit
2D-area	79.206		80.073	+ 1. 09	Low multiplicity of the common cell = 2×{100}KCl
	2×d_{200} = 6.292		3×d_{202} = 5.826	– 7.99	Absorption not hindered, but d_{202} slices of $PbCl_2$ show a strong S character
{100}	$[1\bar{1}0]$ = 8.899	**{110}**	2×[001] = 9.069	+1.91	Low misfit
	4× [110] = 35.60		3× $[1\bar{1}0]$ =35.484	–0.323	Very low misfit
2D area	316.826		321.831	+1.58	Multiplicity of the common cell = 8×(100)KCl
	2×d_{200} = 6.293		d_{110} = 5.828	–7.97	Absorption not hindered

Table 2a. Lattice coincidences between the {100} KCl form and the {001}, {010}, {100}, {101} and {110} $PbCl_2$ forms.

Table 2a shows the lattice coincidences between the KCl cube and the most important forms of $PbCl_2$. It follows that :

- {001} and {010} forms of $PbCl_2$ cannot yield 2D-lattice coincidences, owing to the high values of their misfits with respect to the host phase.
- Instead, very good lattice coincidences occur at the interfaces: {100}-KCl/{101}- and {100}-$PbCl_2$. Nevertheless, when analyzing more closely the features of these coincidence lattices, severe drawbacks are encountered for epitaxy to occur. In fact, the surface profile of the {101}-$PbCl_2$ is highly unstable, due to its strong stepped character shown within the slice of thickness d_{202} (see, for details, Fig.3a S.I.). Moreover, the surface profile of the {100}-$PbCl_2$ is highly wavy (Fig.3b S.I.) and hence cannot easily adhere, even relaxed, to the {100}-KCl substrate, as we will demonstrate through energy calculation in a forthcoming paper.
- Finally, a few words should be spent on the {100}-KCl/{110}-$PbCl_2$ coincidence lattice: in this case, the parametric misfit is exceptionally good, but the area of the common 2D-cell is eight times that of the {100}-2D cell of KCl. This means that the occurrence probability of the corresponding epitaxy should be very low, as it ensues from the general theory of the coincidence lattices,[18] and from our preceding investigations about twins,[19] polytypes and periodic polysynthetic twins.[20]

Summing up, both geometric and structural conditions for {100}-KCl/$PbCl_2$ two dimensional epitaxy to occur can be hardly fulfilled. Hence, we could reasonably conclude that $PbCl_2$ does not contribute to decrease the value of the specific surface energy of the {100}-KCl form. Once demonstrated that $PbCl_2$ can affect neither the equilibrium nor the growth kinetics of the KCl cube, it remains to show how the opposite can occur for the {111} form.

Crystal form (host) KCl	2D-lattice of the host form	Crystal form (guest) $PbCl_2$	2D-lattice of the guest form	2D- misfit (host/guest) Δ%	Notes
{111}	$[1\bar{1}0]$ = 8.899	{001}	[010] = 9.045	+1.63	Low misfit
	½ $[11\bar{2}]$ = 7.707		[100] = 7.622	–1.10	Low misfit
2D-area	68.594		68.941	+ 0. 506	Very low multiplicity of the common cell = 1×(111)KCl
	$4\times d_{111}$ = 14.532		$3\times d_{001}$ =13.604	–6.81	
	$5\times d_{111}$ =18.165		$4\times d_{001}$=18.139	–0.14	Absorption not hindered
{111}	½ $[11\bar{2}]$ = 7.707	{010}	[100] = 7.622	–1.10	Low misfit. {010} a perfect cleavage and the most important form of cotunnite morphology. [21]
	½$[1\bar{1}0]$ = 8.899		2× [001] = 9.070	+1.90	Low misfit
2D-area	68.594		69.120	+ 0. 781	Very low multiplicity of the common 2D cell 2×(010)$PbCl_2$ ≡1×(111)KCl
	$4\times d_{111}$ = 14.532		$3\times d_{020}$ =13.717	–5.94	
	$5\times d_{111}$ =18.165		$4\times d_{020}$=18.289	+0.68	Absorption not hindered
{111}	$[1\bar{1}0]$ = 8.899	{100}[a]	[010] = 9.045	+1.63	Low misfit
	2×$[11\bar{2}]$ =30.83		7× [001] =31.745	+2.97	Low misfit
2D-area	274.379		287.133	+4.65	Medium multiplicity of the common cell 7×(100)$PbCl_2$ ≡ 4×(111) KCl
	d_{111}=3.633		*d_{200}* = 3.811	+4.9	Very easy absorption
{111}	$[1\bar{1}0]$ = 8.899	{100}[b]	2× [001] = 9.070	+1.90	Low misfit
	3×$[11\bar{2}]$ =46.245		5× [010] = 45.225	–2.25	Low misfit
2D-area	411.568		410.191	–0.33	Medium-high multiplicity of the common cell 10×(100)$PbCl_2$ ≡ 6×(111)KCl
	d_{111}=3.633		*d_{200}* = 3.811	+4.9	Very easy absorption
{111}	$[1\bar{1}0]$ = 8.899	{101}[a]	$[10\bar{1}]$ =8.853	–0.53	Very low misfit
	3×$[11\bar{2}]$ =46.245		5× [010] = 45.225	–2.25	Low misfit
2D-area	411.568		400.363	–2.80	Medium-high multiplicity of the common cell 5×(101)$PbCl_2$ ≡ 6 ×(111)KCl
	d_{111}=3.633		d_{101} =3.897	+7.27	Easy absorption
{111}	$[1\bar{1}0]$ = 8.899	{101}[b]	[010] =9.045	+1.63	Low misfit
	3×$[11\bar{2}]$ =46.245		5×$[10\bar{1}$]=44.264	–4.47	Low misfit
2D-area	411.568		400.372	–2.79	Medium-high multiplicity of the common cell 5×(101)$PbCl_2$ ≡ 6 ×(111)KCl
	d_{111}=3.633		d_{101} =3.897	+7.27	Easy absorption
{111}	$[1\bar{1}0]$ = 8.899	{110}[a]	2× [001] = 9.070	+1.91	Low misfit
	3×$[11\bar{2}]$ =46.245		4× $[1\bar{1}$ 0]=47.312	+2.3	Low misfit
2D-area	411.568		429.12	+4.26	Medium-high multiplicity of the common cell 8×(110)$PbCl_2$ ≡ 6×(111)KCl
	$5\times d_{111}$ =18.165		$3\times d_{110}$ =17.485	–3.88	Absorption not-hindered
{111}	4× $[1\bar{1}0]$ = 35.60	{110}[b]	3× $[1\bar{1}$ 0]=35.484	–0.3	Very low misfit
	3×$[11\bar{2}]$ =46.245		10× [001] =45.35	–1.98	Low misfit
2D-area	1646.27		1609.128	–2.30	Very high multiplicity of the common cell 30×(110)$PbCl_2$ ≡ 24×(111)KCl
	$5\times d_{111}$ =18.165		$3\times d_{110}$ =17.485	–3.88	Absorption not-hindered

Table 2b. Lattice coincidences between the {111}-KCl form and: {001}, {010}, {100}, {101} and {110}-$PbCl_2$ forms.

From Table 2b it comes out that both {001} and {010} forms of $PbCl_2$ largely fulfil the geometric conditions for a very good 2D epitaxy on the KCl octahedron. As a matter of fact, all the misfits of the 2D interface meshes do not reach 2%; further, the multiplicity of the common 2D cells assumes the minimum value in both cases: decidedly, this plays in favor of a very good epitaxial adsorption. Concerning the remaining coincidences:

i) the interface {111}-KCl/{100}[a]-$PbCl_2$, shows low parametric misfits and medium multiplicity of the common cell; moreover the d_{200} adsorbed layers can be easily absorbed in the {111}-KCl growth sectors, owing to the small difference between their thickness and that of the d_{111} - KCl steps;

ii) the other epitaxial interfaces related to the: {100}[b], {101} and {110} forms are less or hardly probable, owing to the medium-high or high multiplicity of their common cells.

Finally, more detailed considerations are needed about the surface structure of both {001} and {010} form of $PbCl_2$, in order to choose which one might be the most appropriate to make epitaxy with the {111}-KCl substrate.

Surface structure of {001} and {010} forms of $PbCl_2$: some comments about the Periodic Bond Chain (PBC) analysis. [21]

The first and unique time the $PbCl_2$ theoretical growth morphology was carried out, dates back to the analysis by Woensdregt and Hartman (W.H.)[22] who calculated the relative attachment energies (E_{att}^{hkl}) of the different {*hkl*} forms using a broken bond model in which to each of the bonds (of length *r*) was assigned an energy that is taken proportional to $1/r^2$. From this work, Table 3 can be drawn, in which the ranking (column 3) of the relative value ($E_{att}^{hkl}/E_{crystallization}$) is compared with the order of morphological importance (column 5) that can be obtained from the well-known geometric Donnay-Harker (D.H.) law. [23]

{hkl} form	E_{att}^{hkl}/E_{cr}	W.H. ranking	d_{hkl} (Å)	D.H. ranking
110	0.2499 (a)		d_{110}=5.828	1
	0.2345 (b)*	1		
010	0.2744 (a)*	2	d_{020}=4.522	2
	0.3567 (c)			
120	0.3155	3	d_{011}=4.064	3
100	0.3377	5	d_{120}=3.925	4
011	0.3216*	4	d_{200}=3.811	5
111	0.3781*	6	d_{111}=3.579	6

Table 3. Comparison between the relative value ($E_{att}^{hkl}/E_{crystallization}$) and the morphological importance order obtained from the Donnay-Harker law. Values (a,b,c) in the second column refer to different surface terminations of the same {hkl} crystal form, while d_{hkl} spacing are those fulfilling the *Pnam* space group extinction rules. The Woensdregt's and Hartman's theoretical growth shape was built by forms marked with an asterisk.

According to Table 3, the agreement between the two sequences is rather good. Three other forms, namely {121}, {211} and {201}, were considered in the W.H. analysis: none

of them, along with {120} and {100} forms, enter the theoretical growth shape of the $PbCl_2$ crystal. Surprisingly, the low index form {001} was not considered, even if its character should be flat, as we will show later on. It is likely that this omission could be due to the constraint imposed by the *Pnam* extinction rules: as a matter of fact, the allowed spacing for the {001} form does correspond to d_{002}=2.267Å, that is a too small thickness of a slice for entering the D.H. ranking.

Owing to the excellent lattice coincidences we just found between {111}-KCl and {001}-$PbCl_2$, the surface features of the {001}-$PbCl_2$ form need to be carefully examined. To this purpose, a [100] projection of the $PbCl_2$ structure has been drawn (Fig. 6) with the aim at finding the PBCs running within a slice of d_{002} thickness. Labels of the atoms and symbols used to describe the PBCs are collected in the Supporting Information.

Chains in the 001 planes: the [100] and [010] PBCs.

The $PbCl_2$ growth units do lye perfectly parallel to the 001 plane of the crystal, one half of them at $z=(1/4)c_0$ and the other half at $z=(3/4)c_0$, these two distributions being symmetry related by the inversion centers. Looking, for instance, at the distribution at $z=(3/4)c_0$, one can see that a type of periodic uninterrupted zig-zag chain of bonds develops in the 001 plane, along the [100] direction:

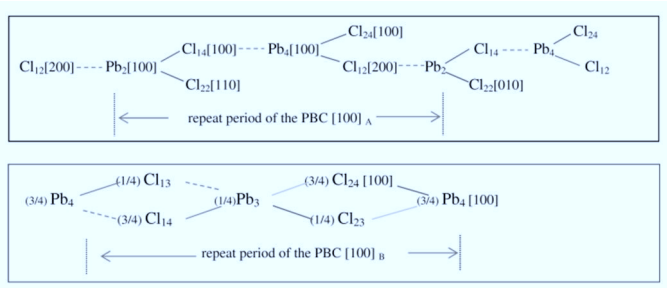

Figure 6. (a) The PBC $[100]_A$, being symmetrical with respect to the glide plane *a*, does not show dipole moment perpendicular to its development axis. All atoms building it, lye in the same 001 plane at $z=(3/4)c_0$. (b) The PBC $[100]_B$, is built by one half of the atoms lying at $z=(1/4)c_0$ and by the other half at $z=(3/4)c_0$.

This chain (Fig. 6a) is stoichiometric and symmetrical with respect to the glide plane *a*, and does not show dipole moment perpendicular to its development axis: then, one can label it as the PBC $[100]_A$. The bonds composing this PBC are: $2\times(\delta_3+\delta_4)$; two strong δ_1 bonds, working as lateral branches of this chain, do not intervene in its structure and hence the PBC $[100]_A$ is a weak one. No other chain links these parallel and contiguous PBCs in the 001 plane and then, at first sight, the character of the {001} form should be stepped (S).

Nevertheless, another PBC can be found along the [100] direction, when both the distributions of growth units at $z=(1/4)c_0$ and $z=(3/4)c_0$ are considered. Three main features characterize this new PBC$[100]_B$:

i) The bonds composing the complete PBC $[100]_B$ are: $2\times(\delta_1+\delta_2+\delta_4+\delta_5)$

ii) The electric dipole moment perpendicular to its development axis vanishes, owing to the symmetry imposed by the inversion centres at (0, ½ , ½) and (½, ½ , ½).

iii) To build a complete period [100], one has to use three atoms lying at $z=(1/4)c_0$ and three other ones at $z=(3/4)c_0$, which means that the PBC belongs to both the 001 planes at $z=(1/4)c_0$ and $z=(3/4)c_0$. As we will see before long, the surface structure of the {001} form should be strongly affected by this constraint.

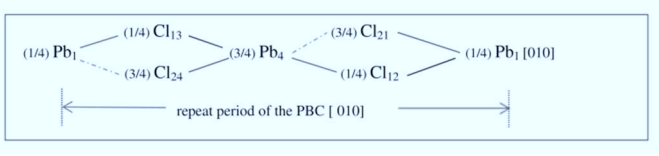

Figure 7. The PBC [010], developing between two 001 planes. A Pb atom, at $z=(1/4)c_0$ coordinates two Cl atoms, at $z=(1/4)c_0$ and $z=(3/4)c_0$, respectively. They, in turn, are coordinated by another Pb atom, at $z=(3/4)c_0$, and so on.

This [010] PBC, drawn in Fig. 7, is composed by the bonds: $2\times(\delta_1+\delta_2+\delta_3+\delta_6)$. It is also not polar, perpendicularly to its development axis, due to the 001 glide *n* planes, at $x=(1/4)a_0$ and $x=(3/4)a_0$. Further, it runs in between the two 001 planes at $z=(1/4)c_0$ and $z=(3/4)c_0$, as previously done by the PBC $[100]_B$.

When coupling the characteristics of both the PBC $[100]_B$ and PBC [010], one can assess that:

- the {001}form should have a good F character, owing to the presence of two PBCs running within a slice of thickness d_{002};
- a d_{002} slice does contain neither the entire plane of $PbCl_2$ units lying at $z=(1/4)c_0$, neither the one at $z=(3/4)c_0$, since in both planes the chains of Pb-Cl bonds are interrupted; as a matter of fact, each of these planes is the frontier between two adjacent d_{002} slices and, consequently, one half of the atoms does belong to a slice and the remaining half to the adjacent one.

Accordingly, the outmost layer of the {001} form should be "spontaneously reconstructed", obeying to the symmetry criterion we successfully started when dealing with {012} surfaces of calcite.[24] Here, we would like to remember that reconstructed surfaces are more sensitive to the tangential relaxation with respect to the unrelaxed ones; in our case this could play in favor of the {001} surfaces which would better compensate the parametric misfit with the {111}-KCl substrate, when compared to the {010} surfaces which don't need to be reconstructed (see Fig. 4 S.I.).

In the next paragraphs we will analyze the geometric coincidences between the KCl crystal and the other potentially crystallizing phases in the Pb-doped growth solution: PbCl(OH), laurionite-paralaurionite and $KCl\cdot 2PbCl_2$, challacolloite.

The KCl / laurionite-PbCl(OH) interfaces.

From Table 4a, it follows that the adsorption of laurionite on the {100}-KCl form could be limited to its {101} form, since

only in this case the geometric constraints for epitaxy can be fulfilled, owing to the low-medium multiplicity of the coincidence 2D cell. Moreover, the character of the {101} laurionite form is markedly flat, as it ensues from our PBC analysis and from the shining aspect of their surfaces.[21] On the contrary, the absorption of the d_{101} laurionite layers into the {100}-KCl growth sectors should not be favored, owing to the very poor short range overlapping of substrate and adsorbate steps.

Crystal form (host) KCl	2D-lattice of the host form	Crystal form (guest) PbCl(OH)	2D-lattice of the guest form	2D- misfit (host/guest) Δ%	Notes
	2×[010] = 12.58	**{101}**	$[10\bar{1}]$= 12.026	– 4.61	Low misfit
	2×[100] = 12.58		3×[010] = 12.061	– 4.31	Low misfit
2D-area	158.27		145.044	9.12	Low-medium multiplicity of the common cell = 4×(100)KCl
	$7\times d_{100}$ = 44.051		$8\times d_{101}$ = 45.88	–4.1	Absorption not favoured
{100}	4× $[1\bar{1}0]$= 35.599	**{010}**	5× [001] = 35.555	– 0.12	Very low misfit
	[110] = 8.899		[100] = 9.698	+ 8.98	Medium misfit
2D-area	316.825		344.833	+ 8.8	Medium-high multiplicity of the common cell = 8×(100)KCl
	$4\times d_{200}$ = 12.584		$3\times d_{010}$ = 12.06	+4.34	Not easy absorption
	4× $[1\bar{1}0]$= 35.599	**{001}**	9× [010] = 36.183	+1.64	Low misfit
	[110] = 8.899		[100] = 9.698	+8.975	Medium misfit
2D-area	316.825		350.921	+10.76	Medium-high multiplicity of the common cell = 8×(100)KCl
	$7\times d_{200}$ = 22.022		$6\times d_{002}$ = 21.33	+3.24	Not easy absorption
	[100] = 6.293	**{100}**	[001] = 7.111	+13.00	Δ% exceeds the limits of 2D epitaxy
	2×[010] = 12.58		3×[010] = 12.061	– 4.31	Low misfit
2D-area	79.17		85.765	+8.33	Low multiplicity of the common cell = 2×(100)KCl
	$3\times d_{200}$ = 9.438		$2\times d_{200}$ = 9.7	+2.77	Not hindered absorption
	4× $[1\bar{1}0]$= 35.599	**{110}**	5× [001] = 35.555	–0.12	Very low misfit
	[110] = 8.899		$[1\bar{1}0]$ = 10.499	+17.96	Δ% exceeds the limits of 2D epitaxy
2D-area	316.825		373.284	+17.80	Low multiplicity of the common cell = 8×(100)KCl
	$6\times d_{200}$ = 18.876		$5\times d_{110}$ = 18.57	–1.65	Not easy absorption

Table 4a. Lattice coincidences between the {100}-KCl form and {101}, {010}, {001}, {100} and {110} forms of laurionite.

Concerning the others forms of laurionite, the geometric conditions for epitaxy do not occur, either for the medium-high multiplicity of the common 2D cells, as for {001} and {010} forms, or for some severe parametric misfits, as for {100} and {110}.

Crystal form (host) KCl	2D-lattice of the host form	Crystal form (guest) PbCl(OH)	2D-lattice of the guest form	2D-misfit (host/guest) Δ%	Notes
{111}	$[1\bar{1}0]$ = 8.899	**{010}**[a]	[100] = 9.699	+8.97	Medium-low misfit
	$[11\bar{2}]$ = 15.415		2×[001] = 14.222	– 8.39	Medium-low misfit
2D-area	137.190		137.935	+ 0. 54	Very low area misfit. Low multiplicity of the common cell = 2× (111)KCl
	d_{111}= 3.633		d_{010} = 4.020	+ 10.66	Absorption slightly favoured
	$[\bar{1}32]$ = 23.546	**{010}**[b]	2×[101] = 24.052	+2.15	Low misfit
	2×$[10\bar{1}]$ = 17.799		$[10\bar{2}]$ = 17.214	–3.4	Low misfit
2D-area	411.569		413.805	+ 0. 54	Very low area misfit. Medium-high multiplicity of the common cell = 6× (111)KCl
	d_{111}= 3.633		d_{010} = 4.020	+ 10.66	Absorption slightly favoured
	$[\bar{2}2\bar{1}]$ = 15.415	**{101}**	4× [010] =16.081	+4.32	Low misfit
	$[11\bar{2}]$ = 15.415		$[\bar{1}21]$ = 14.466	–6.56	Low misfit
2D-area	205.78		193.39	–6.40	Low area misfit. Low multiplicity of the common cell = 3× (111)KCl
	$3\times d_{111}$= 10.899		$2\times d_{101}$ = 11.47	+5.24	Absorption favoured
	$[1\bar{1}0]$ = 8.899	**{001}**	[100] = 9.699	+8.97	Medium misfit
	$[11\bar{2}]$ = 15.415		4× [010] =16.081	+4.32	Low misfit
2D-area	137.190		155.966	+13.68	Medium area misfit. Low multiplicity of the common cell = 2× (111)KCl
	d_{111}= 3.633		d_{002}= 3.555	–2.18	Absorption highly favoured
	$[\bar{2}11]$ = 15.415	**{100}**	4× [010] =16.081	+4.32	
	4×$[01\bar{1}]$ = 35.599		5×[001] = 35.555	–0.12	
2D-area	548.726		571.760	+4.20	Low area misfit. High multiplicity of the common cell = 8× (111)KCl
	$4\times d_{111}$= 14.532		$3\times d_{200}$ = 14.5485	+0.11	Absorption favoured
	3×$[1\bar{1}0]$ = 26.994	**{110}**	4× [001] = 28.44	+5.35	Low misfit
	2×$[11\bar{2}]$ = 30.828		3× $[1\bar{1}$ 0]=31.497	+2.17	Low misfit
2D-area	832.171		895.774	+7.64	Low area misfit. High multiplicity of the common cell = 12× (111)KCl
	d_{111}= 3.633		d_{110} = 3.714	+2.23	Absorption highly favoured

Table 4b. Lattice coincidences between the {111}-KCl form and: {010}, {101}, {001}, {100} and {110} forms of laurionite.

Table 4b illustrates the coincidences lattices between the {111}-KCl form and laurionite.

It follows that epitaxial adsorption of laurionite on the {111}-KCl form is highly favored and that absorption of adsorbed layers into the {111}-KCl growth sectors can also occur in one half of the considered cases, at least. In fact:

i) Very short range coincidences are obtained for {010}[a], {001} and {101} forms of laurionite, while medium-long range coincidence lattices can be found for {010}[b], {100} and {110} forms. Thus, geometric constraints for 2D-epitaxy to occur at the $\{111\}_{KCl}$ / laurionite interface, are largely fulfilled.

ii) Adsorbed laurionite layers of the {001} and {110}forms can be very easily buried into the $\{111\}_{KCl}$ growing faces. Moreover, the absorption of {101} and {100} laurionite layers has good probability to occur, while increasing difficulty is encountered to bury the adsorbed {010} layers.

Summing up, one has the certainty that when KCl crystals grow in an aqueous solution, supersaturated with respect to KCl and unsaturated with respect to PbCl(OH), an ordered adsorption of 2D islands of PbCl(OH) widely prevails on the octahedron with respect to the cube faces of KCl crystals. From the kinetic point of view, on the octahedron surfaces the KCl layers (which try to propagate on the fresh surfaces) will compete with the adsorbed PbCl(OH) islands (which try to occupy the fresh surfaces, as much as the Pb concentration increases in the mother solution). Consequently, adsorbed laurionite layers are added to the cotunnite ones in determining the {100} → {100}+{111} habit change of KCl crystals when growing from Pb doped aqueous solutions.

Investigating lattice coincidences between {111}-KCl and PbCl(OH), para-laurionite, should be considered as pleonastic, owing to the close lattice relationships between laurionite (L) and para-laurionite (PL). As a matter of fact, these two structures can be viewed as polytypes belonging to the MDO (Maximum Degree of Order) category, according to Merlino et al. [25] From the control on their parametric fits it follows that:

i) $[301]_{PL}$= 28.984 Å, while $3\times[100]_L$ = 29.096 Å, the percent misfit being +0.39;

ii) $[001]_{PL}$= 7.233 Å , while $[001]_L$= 7.111 Å, with a misfit of -1.72;

iii) $2D_{PL}$ - mesh area = 209.613 $Å^2$, while $2D_L$ - mesh area = 206.902 $Å^2$, the misfit being +1.31.

These quasi-perfect coincidences between the lattices of laurionite and para-laurionite allow to say that the epitaxy between {111}-KCl and para-laurionite should be as good as those just estimated between {111}-KCl and {010}, {101} and {001} forms of laurionite.

The KCl / challacolloite-KCl·2PbCl interfaces

Table 5 illustrates the lattice coincidences between {001} and {111} forms of KCl and the morphologically most important forms of challacolloite.[26] It comes out that the lattice coincidences between challacolloite and the KCl cube are largely unfavorable, since the minimum of the multiplicity of the 2D-common cell, equal to $8\times(001)_{KCl}$, is reached for the {111}KCl/{010}-challacolloite interface. On the contrary, very low and low multiplicities are obtained between the {111}-KCl form and {001} and {111} forms of challacolloite, respectively. Further, it is worth outlining that the shape of the 2D-coincidence cell of the {111}-KCl/{001}-challacolloite interface deviates by only 0.81° from the perfect hexagonality, which fully agrees with the trigonal symmetry of the {111}-KCl surfaces.

Crystal form (host) KCl	2D-lattice of the host form	Crystal form (guest) $KCl{\cdot}2\,PbCl_2$	2D-lattice of the guest form	2D- misfit (host/guest) Δ%	Notes
{001}	$[1\bar{1}0]$ = 8.8998	**{001}**	[100] = 8.864	– 0.004	Very low misfit
	8× [110] = 71.984		9× [010] = 71.388	–0.83	Very low misfit
2D-area	640.643		632.783	–1.22	Very low area misfit. High multiplicity of the common cell = 16×(001)KCl
	d_{001} = 6.293		d_{002} = 6.245	–0.77	Absorption highly favoured
	$[1\bar{1}0]$ = 8.8998	**{010}**	[100] = 8.864	– 0.004	Very low misfit
	4×[110] = 35.599		3× [001] =37.473	+5.26	Low misfit
2D-area	316.826		332.161	+4.85	Low area misfit. Medium-high multiplicity of the common cell = 8×(001)KCl
	$2\times d_{001}$ = 12.586		$3\times d_{020}$ = 11.898	-5.78	Absorption slightly favoured
	2× [010] =12.586	**{100}**	[001]=12.49	-0.77	Very low misfit
	5× [100] =31.465		4× [010] =31.728	+0.83	Very low misfit
2D-area	396.018		396.282	+0.067	Very low area misfit Medium-high multiplicity of the common cell = 10×(001)KCl
	$2\times d_{001}$ = 12.586		$3\times d_{200}$ = 13.296	+5.64	Absorption slightly favoured
	5× [010] = 31.465	**{102}**	4× [010] =31.728	+0.83	Very low misfit
	7× [010] = 44.051		2× $[\bar{2}01]$ =43.3728	-1.56	Low misfit
2D-area	1386.064		1376.138	– 0.72	Very low area misfit. Very high multiplicity of the common cell = 35×(001)KCl
	$4\times d_{001}$ = 25.172		$5\times d_{102}$ = 25.525	+1.4	Absorption slightly favoured
{111}	$[1\bar{1}0]$ = 8.8998	**{001}**	[100] = 8.864	– 0.004	Very low misfit
	½ $[11\bar{2}]$ = 7.7074		[010] = 7.932	+ 2.91	Low misfit
2D-area	68.5943		70.3092	+ 2.50	Very low area misfit. Cell obliquity with respect to hexagonality = 0.805°. Very low multiplicity of the common cell = 1×(111)KCl
	$7\times d_{111}$ = 25.431		$4\times d_{002}$ = 24.98	– 1.8	Absorption very slightly favoured
	$[11\bar{2}]$ = 15.415	**{100}**	$[0\bar{1}1]$ = 14.796	+ 4.18	Low misfit
	$[\bar{1}2\bar{1}]$ = 15.415		[011] = 14.796	+ 4.18	Low misfit
2D-area	205.787		198.141	– 3.86	Low area misfit. Cell obliquity with respect to the hexagonality = 4.83° Low multiplicity of the common cell = 3×(111)KCl
	$5\times d_{111}$ = 18.165		$4\times d_{200}$ = 17.728	– 2.46	Absorption slightly favoured
	3× $[01\bar{1}]$ = 26.70	**{010}**	2× [001] =24.982	–6.87	Medium-low misfit
	$[\bar{2}11]$ = 15.415		2× [100] = 17.728	+15	Very high parametric misfit
2D-area	411.571		442.881	+7.6	Low area misfit. Medium multiplicity of the common cell = 6×(111)KCl
	d_{111} = 3.633		d_{020}=3.966	+9.16	Absorption favoured
	$[11\bar{1}]$ = 15.415	**{102}**	2× [010] = 15.864	+2.9	Low misfit
	5× $[1\bar{2}0]$ = 44.499		2× $[\bar{2}01]$ =43.3728	–2.59	Low misfit
2D-area	685.952		688.066	+0.31	Very low area misfit Medium-high multiplicity of the

$4\times d_{111}$ =14.532	$3\times d_{102}$ =15.315	-5.39	common cell = 10×(111)KCl Absorption slightly favoured

Table 5. Lattice coincidences between {001} and {111} forms of KCl and {001}, {010}, {100} and {102} forms of challacolloite KCl·2 $PbCl_2$

Summing up, also in this case, the adsorption on the KCl octahedron is highly favored with respect to that on the cube. Concerning the absorption, challacolloite layers undergo some difficulties to be buried in the {111}-KCl growth sectors, except for the {111}-KCl/{010}-challacolloite interface. Instead, absorption could be highly favored in the {001}-KCl growth sectors, since the thicknesses of the competing KCl and challacolloite elementary layers fit very well (host/guest misfit of 0.77%), as it occurs at the {001}-KCl/{001}-challacolloite interface; contrarily, the probability of this epitaxy to occur should be very low, since the corresponding 2D-common cell is associated to a very high multiplicity, equal to 16×(001)KCl .

Discussion and conclusions

According to the partial and preliminary considerations just drawn from Tables 2, 4 and 5, an order of priority could be proposed about the probability of 2D epitaxy between KCl crystals and the compounds that could potentially crystallize from Pb doped solutions:

a) The KCl octahedron is largely favoured, with respect to the cube, for epitaxially adsorbing all the examined compounds. This implies that the ratio between $\{111\}_{KCl}$ and $\{001\}_{KCl}$ interfacial energies strongly reduces, up to a point that the octahedron might enter the equilibrium shape of KCl. Consequently, the Pb adsorption can work since the early stages of KCl nucleation and then the relative normal growth rate of the two competing forms, $R_{\{111\}}/R_{\{001\}}$, can decrease as much as the Pb concentration increases in the mother solution. Our kinetic considerations are supported by remembering that: i) the normal growth kinetics $R_{\{111\}}$ and $R_{\{001\}}$ of the F faces {111} and {001} is ruled by the advancement rate of the macro-steps shown in Fig. 4 and in the S.I. The structure of these macro-steps is the same for both the growing {111} and {001} forms in the presence of Pb, as we illustrated in section 2.3.; ii) thus, they could run at the same rate, if the inter-step terraces would have the same structure on both cube and octahedron surfaces; iii) but the octahedron terraces can be strongly affected by the epitaxial adsorption, as we just proposed, and then the macrosteps spreading on {111} surfaces should be markedly hindered with respect to that of the cube; iv) consequently, Pb adsorption progressively enhances the normal growth rate ratio $R_{\{001\}}/R_{\{111\}}$, which explains the observed morphology change from {001} → {001}+{111} → {111}.

b) Concerning the potential epitaxies:

i) The case $\{111\}_{KCl}/\{010\}_{PbCl2}$ seems to be most favored, owing to the F character of the $\{010\}_{PbCl2}$ form, while the case $\{111\}_{KCl}/\{001\}_{PbCl2}$ seems to be less probable, due the K/S character of $\{001\}_{PbCl2}$. Besides, in both cases the multiplicity of the coincidence cell is very small, its minimum value being reached for the $\{111\}_{KCl}/\{010\}_{PbCl2}$ interface, where the corresponding 2D area coincides with a half of the $\{111\}_{KCl}$ cell. Moreover, the percent misfit of the common areas is 0.78 and 0.50 for $\{111\}_{KCl}/\{010\}_{PbCl2}$ and $\{111\}_{KCl}/\{001\}_{PbCl2}$, respectively, which means that the relaxation needed to adapt the KCl and $PbCl_2$ structures at the epitaxial interface should be necessarily low.

ii) The good coincidences found between $\{111\}_{KCl}$ and the $\{010\}^{a}$, {001} and {101} forms of laurionite account for a competition between cotunnite and laurionite-paralaurionite to increase the morphological importance of the KCl octahedron.

iii) Also the case {111}-KCl/{001}-challacolloite has a good chance to occur. In fact:

- The character of the {001} form of KCl·2 $PbCl_2$ is decidedly F, as we will detail in a forthcoming special paper devoted to the quantitative equilibrium shape of cotunnite, laurionite and challacolloite.
- Further, the slices of thickness d_{002}, allowed by the extinction rules, are centre-symmetric and their surface profile cannot need to be reconstructed, since the contiguous d_{002} slices are related by the arrays of the 2_1 diad axes.
-The obliquity of the 2D cell of KCl·2 $PbCl_2$ is negligible, since it only deviates by 0.805° from the perfect A_3 symmetry of the {111}-KCl substrate. Having also considered the small misfit (2.5%) of the common mesh along with its very low multiplicity, one can easily foresee that, for epitaxy to occur, a non-relevant relaxation should be needed at this epitaxial KCl/challacolloite interface.

c) A last consideration, concerning the Pb absorption in the KCl crystal bulk, comes out from Tables 2, 4 and 5. The octahedron largely prevails on the cube in burying the adsorbed epi-layers containing Pb. In fact, only in one case ($\{001\}_{KCl}/\{100\}_{KCl\cdot 2PbCl2}$) lead could be very easily absorbed in the cube growth sector, even if the coincidence lattice is affected by a very high multiplicity. Laurionite-paralaurionite largely favor the Pb absorption in the $\{111\}_{KCl}$ growth sectors, especially in the cases: $\{111\}_{KCl}/\{001\}_{PbCl(OH)}$ and $\{111\}_{KCl}/\{100\}_{PbCl(OH)}$; instead, cotunnite can favor the Pb capture only at the interface $\{111\}_{KCl}/\{100\}_{PbCl2}$, while challacolloite can be hardly absorbed.

When summarising, we proposed an epitaxial path to interpret both the morphological habit change of KCl in Pb doped aqueous solution and the consequent selective absorption of Pb in the growth sectors of the KCl octahedron. This way seems to be promising and we are quantitatively improving our investigation, by X-ray diffraction and by calculating the adhesion energies involved in the best of the lattice coincidences we found. Our final aim is to verify, in a forthcoming paper, if the adsorbed foreign layers are able to generate anomalous mixed crystals like those we recently found in the systems: $CaCO_3$ (calcite)/(Li_2CO_3) zabuyelite and NaCl (halite)/H-CO-NH_2 (formamide)[27].

References

1 P. Gaubert, Compt. Rend. Académ. Sci. Paris, 1925, **180**, 378.
2 C.W. Bunn, Proc. Roy.Soc., 1933, **A 141**, 567.
3 L. Royer, Compt. Rend. Académ. Sci. Paris, 1934, 198: a) 185 ; b) ibid. 585 ; c) ibid. 949 ; d) ibid. 1868 ; e) see an excellent summary by P. Hartman, in « Adsorption et Croissance Cristalline » Coll. Internat. CNRS, n° 152, Ed. R. Kern, 1965, 477.
4 J.W. Retgers, Z. Physik. Chem. 1982, **9**, 267.
5 R. Kern, Bull. Soc. Franç. Mineral. Crist. 1953, **76**, 391
6 H.E. Buckley, Crystal Growth, 1958 (Wiley, New York)
7 M. Bienfait, R. Boistelle, R. Kern, in « Adsorption et Croissance Cristalline » Coll. Intern. CNRS bn° **152**, Paris, 1965, pg.577
8 Y. Aoki, J. Japan. Assoc. Mineral. Petrol. Econ. Geol., 1982, Spec. Issue **3**, 123 (in Japanese)
9 T. Nishida, Surface 1986, **24**, 197, in Japanese
10 L. Lian, K. Tsukamoto, I. Sunagawa, J. Crystal Growth 1990, **99**, 150.
11 P. Hartman, W.G. Perdok, Acta Cryst. 1955, **8**: I, 49-52; II, ibid. 521-524; III, ibid. 525-529.
12 L. Pastero, E. Costa, M. Bruno, M. Rubbo, G. Sgualdino, D. Aquilano, Crystal Growth & Design, 2004, **4**, 485.
13 a) E. Bittarello, F.R. Massaro, M. Rubbo, D. Aquilano, Crystal Growth & Design. 2009, **9**(2), 971; b) E. Bittarello, F.R. Massaro, Aquilano, J. Crystal Growth 2010, **312**, 402.
14 L. Pastero, D. Aquilano, M. Moret, Crystal Growth & Design, 2012, **12** (5), 2306.
15 M. Bruno, D. Aquilano, L. Pastero, M. Prencipe, Crystal Growth & Design, 2008, **8** (7), 2163.
16 D. Aquilano, L. Pastero, M. Rubbo, J. Crystal Growth, 2009, **311**, 399.
17 a) M. Bienfait, R. Kern, Bull. Soc. Franç. Minéral. Cristall. 1964, **87**, 604; b) R. Kern, "The equilibrium form of a crystal" in Morphology of crystals, Part A, I. Sunagawa Ed., Terra Sci. Publ.Co./Tokyo, D. Reidel Publ.Co./Dordrecht, 1987, Ch.2, 77-206.
18 W. Bollmann, Crystal Defects and Crystalline Interfaces (Berlin, Springer) 1970.
19 M. Bruno, F.R. Massaro, M. Rubbo, M. Prencipe, D. Aquilano, Cryst. Growth & Design, 2010, **10**, 3102.
20 R. Boistelle, D. Aquilano, Acta Cryst., 1977, **A33**, 642.
21 P. Groth, Chemische Krystallographie, Engelmann, Leipzig 1906, **Vol.1**, pg 219- 220, 297
22 C.F. Woensdregt, P. Hartman, J. Crystal Growth 1988, **87**, 561.
23 J.D.H. Donnay, D. Harker, Am. Mineralogist 1937, **22**, 446
24 a) F.R. Massaro, L. Pastero, M. Rubbo, D. Aquilano. J. Crystal Growth 2008, **310**, 706. b) M. Bruno, F.R. Massaro, M. Prencipe, Surface Science, 2008, **602**, 2774.
25 S. Merlino, M. Pasero, N. Perchialli, Mineral. Magazine, 1993, **57**, 323.
26 J. Schlüter, D. Pohl, S. Britvin, N. Jb. Miner. 2005, Abh. **182**(1), 95.
27 D. Aquilano, L. Pastero, Anomalous mixed crystals: a peculiar case of adsorption/absorption, in International School "Adsorption, Absorption and Crystal Growth", Cryst. Res. Technol. 2013, **48**, 819-839.